

Contents lists available at ScienceDirect

Journal of Energy Chemistry

JOURNAL OF ENERGY CHEMISTRY

http://www.journals.elsevier.com journal-of-energy-chemistr

journal homepage: www.elsevier.com/locate/jechem

Sulfonic groups functionalized Zr-metal organic framework for highly catalytic transfer hydrogenation of furfural to furfuryl alcohol

Jingcheng Wu^{a,b}, Dong Liang^b, Xiangbo Song^c, Tingsen Liu^c, Tianyi Xu^a, Shuangyin Wang^a, Yuqin Zou^{a,b,*}

- ^a State Key Laboratory of Chem/Bio-Sensing and Chemometrics, Advanced Catalytic Engineering Research Center of the Ministry of Education, College of Chemistry and Chemical Engineering, the National Supercomputer Centers in Changsha, Hunan University, Changsha 410082, Hunan, China
- ^b Shenzhen Institute of Hunan University, Shenzhen 518057, Guangdong, China
- ^c School of Physical and Electronic Sciences, Chuxiong Normal University, Chuxiong 675099, Yunnan, China

ARTICLE INFO

Article history: Received 26 January 2022 Revised 23 February 2022 Accepted 24 February 2022 Available online 5 March 2022

Keywords: Hydrogenation Biomass Metal organic framework Biorefinery

ABSTRACT

The highly selective catalytic transfer hydrogenation (CTH) of furfural (FF) to furfuryl alcohol (FOL) is a significant route of biomass valorization. Herein, a series microporous Zr-metal organic framework (Zr-MOF) functionalized by sulfonic groups are prepared. Based on the comprehensive structural characterizations by means of X-ray diffraction (XRD), scanning electron microscopy (SEM), transmission electron microscopy (TEM), N2 physisorption, Thermogravimetric (TG) and Fourier transformed infrared spectroscopy (FTIR), we find that sulfonic acid (-SO₃H) functional groups are tethered on the UIO-66 without affecting the structure of the framework. Systematic characterizations (NH₃-TPD, CO₂-TPD, and in-situ FTIR) demonstrate that modifying of sulfonic groups on UIO-66 results in the formation of stronger Lewis acidic-basic and Brønsted acidis sites. The cooperative role of the versatile Lewis acidic-basic and Brønsted acidic sites in 60% mol fraction of sulfonic acid-containing UIO-66 (UIO- $S_{0.6}$) retain high surface area and exhibit excellent catalytic performance of 94.7% FOL yield and 16.9 h^{-1} turnover number (TOF) under mild conditions. Kinetic experiments reveal that the activation energy of the CTH of furfural (FF) over UIO- $S_{0.6}$ catalyst is as low as 50.8 kJ mol⁻¹. Besides, the hydrogen transfer mechanism is investigated through isotope labeling experiments, exhibiting that the β -H in isopropanol is transferred to the α -C of FF by forming six-membered intermediates on the Lewis acidic-basic and Brønsted acidic sites of the UIO-S_{0.6}, which is the rate-determining step in the formation of FOL.

© 2022 Science Press and Dalian Institute of Chemical Physics, Chinese Academy of Sciences. Published by ELSEVIER B.V. and Science Press. All rights reserved.

1. Introduction

The efficient upgrading of inexhaustible nonfood lignocellulosic biomass to bio-fuels and value-added products has obtained increasing attention as a means to substitute traditional fossil resources [1,2]. More recently, catalytic transfer hydrogenation (CTH) of biomass-derived aldehydes to the corresponding alcohols, employing organic alcohols or acids as the hydrogen donor to replace dangerous H₂, is an alternative strategy for the upgrading of renewable biomass-derived platform chemicals to bio-fuels and value-added products [3,4]. Among these biomass-derived aldehydes, furfural (FF) and 5-hydroxymethylfurfural (5-HMF) could be directly gained from cellulose and hemicellulose, respectively [5–7]. Selectively hydrogenation FF into furfuryl alcohol (FOL) is of great significance in biorefinery because FOL is eventful

intermediates extensive exploited in the production of crown ethers, adhesives, furan-based resins, artificial fibers, fuels, and fuel additives [8,9].

Although some precious metal catalysts, such as Ru and Rh, exhibited high catalytic performance for the CTH, their usage is confined dramatically in practical application due to its high cost [10,11]. Therefore, developing non-precious metal-based catalysts with low prices is highly desirable for upgrading FF in practical applications. Recently, Zr-based zeolites as Lewis acidic materials have been prepared to achieve CTH reactions [12,13]. In this process, acidic sites on the surface of Zr-based zeolites would weaken the –OH bond in alcohols and carbonyl groups [14,15]. Simultaneously, the corresponding primary sites could attract hydrogen from alcohols, resulting in the formation of an alkoxide adsorbed on the adjacent Lewis acid site, and thus promoting the hydrogen transfer [16-18].

UIO-66 is a Zr-based organic framework material, which has aroused intensive research interest owing to its intrinsic

^{*} Corresponding author.

E-mail address: yuqin_zou@hnu.edu.cn (Y. Zou).

advantages, such as the tunable structure and physicochemical properties [19]. UIO-66 has a high level of Lewis acidic sites, which is expected to accelerate the hydrogenation of various carbonyl compounds to the corresponding alcohols without gasous H₂. Notably, the high surface area and porosity of UIO-66 could also provide a large amount of accessible active sites, which possess tremendous potential for the improvement of catalytic performance [20,21]. Unfortunately, UIO-66 exhibited low catalytic performance in the CTH of FF to FOL due to the low basic sites and Brønsted acidic sites. Therefore, introducing stronger basic sites and Brønsted acidic sites to adjacent the Lewis acidic sites on UIO-66, which significantly enhanced the catalytic performance.

Herein, various sulfonic groups functionalized UIO-66 (UIO-S_{x.} x is 0.2, 0.4, 0.6 and 0.8) were prepared by using a one-step, bottomup method. The structure and physical-chemical properties of UIO-S_x catalysts was characterized to prove the coordination between sulfonic groups and the UIO-66 frameworks, suggesting the obtained UIO-S_x with porous frameworks after incorporating the number of sulfonic groups could remarkably enhance the Lewis acidic-basic and Brønsted acidic sites and therefore promote the catalytic performance. Optimizations of the CTH reaction parameters and the kinetic experiments were also performed. To further study the reaction mechanism, the combination of hydrogen donor experiments, deuterium isotope labeling experiments, mass fragmentation analysis (MS), and ¹H nuclear magnetic resonance (NMR) were performed. The role of acidic and basic sites in mediating the CTH reaction pathway at the molecular level was discussed. Furthermore, the recycling experiments were conducted to study the reusability of the catalysts.

2. Results and discussion

The sulfonic acid (-SO₃H) functionalized UIO-66 (UIO-S_x) was synthesized by a hydrothermal method. Firstly, the UIO-S_x catalysts are characterized by XRD, diffraction peaks at 2θ of 7.36°, 8.48°, and 25.68° are observed in the XRD patterns for UIO-S_x catalysts, which are attributed to (1 1 1), (0 0 2), and (1 1 5), respectively (Fig. 1a). These peaks are slightly shifted compared with UIO-66, suggesting the functionalization of the frameworks of UIO-66 by sulfonic groups [22]. Then, SEM and transmission electron microscopy (TEM) images exhibit that UIO-S_{0.6} is composed of uniformly stacked nanosheets, which are about 200 nm (Fig. 1b-d). N₂ adsorption and desorption isotherm of UIO-S_{0.6} exhibits a typical IV-type isotherm with hysteresis loops in Fig. S1, indicating the presence of porous structure in UIO-S_{0.6} catalyst. Table S1 shows that UIO- $S_{0.6}$ has a high surface area (795.9 m² g⁻¹) and large pore volume (9.5 cm³ g⁻¹). Thermogravimetric (TG) is conducted to study the excellent thermal stability of UIO-S_{0.6} at the reaction conditions (Fig. 1e, Fig. S2). The weight of UIO-S_{0.6} has a slight loss below 112 °C, which may be attributed to the desorption of water. There is a steep decrease from 460 °C to 560 °C, suggesting the faster weight loss in this stage, attributed to the pyrolysis of the oxygen group of UIO-S_{0.6}.

The oxidation state of UIO-66 and UIO- $S_{0.6}$ catalysts were characterized by X-ray photoelectron spectroscopy (XPS). In the XPS spectra of UIO- $S_{0.6}$ (Fig. 1f), Zr $3d_{5/2}$ and $3d_{3/2}$ firm peaks at 182.58 and 184.98 eV are shifted to a lower level (182.18 and 184.58 eV) in comparison with UIO-66, suggesting that the higher positive charge of Zr in UIO- $8_{0.6}$ and thus stronger acidic and basic sites are formed in UIO- $8_{0.6}$ [23]. Besides, the binding energy of O 1 s assigned to Zr-O-Ar (Ar, benzene ring) interaction in UIO- $8_{0.6}$ is higher than Zr-O-Zr in ZrO₂ (Fig. 1g). The O atom in UIO- $8_{0.6}$ is declared a medium base strength, attributed to the negative charge on the O atom. The XPS results demonstrate that the O atom in UIO- $8_{0.6}$ is worked as the basic site to balance the Lewis acid sites

 Zr^{4+} , which will conduct the -Ar-O-Zr-O-Ar- groups in metal-organic frameworks. The S 2p peaks showed that the binding energy at 167.6 and 168.7 eV which are assignable to S $2p_{3/2}$ and $2p_{1/2}$ of – SO₃H groups (Fig. S3).

The acid-base properties of UIO- $S_{0.6}$ and UIO-66 were also studied by NH₃-TPD and CO₂-TPD (Fig. 1h and i). The increased desorption temperature of CO₂ and NH₃ demonstrated the significant enhancement in density and strength of basic and acidic sites in UIO- $S_{0.6}$ after functionalizing sulfonic groups with UIO-66. The acid-base density of UIO- $S_{0.6}$ and UIO-66 are shown in Table S2. The acidic and basic sites of UIO- $S_{0.6}$ are attributed to the coordination of terephthalic acid hydroxyl and Zr, facilitating the formation of -Ar-C-O-Zr-O-C-Ar- frameworks [24].

The transmission FTIR was performed to investigate the modification of functional groups on UIO-S_{0.6} (Fig. 2a and b). A series bands at 1656, 1582, and 1401 cm⁻¹, which attributed to the asymmetric and symmetric vibration of C=O bond, are observed in both FTIR spectra of UIO-66 and UIO-S_{0.6}. The bands at 1075 and 1025 cm⁻¹ are attributed to the C-O bond in both UIO-66 and UIO-S_{0.6}. Also, bands at 747 and 668 cm⁻¹ are attributed to the mix of -OH and -CH bending mode and Zr-O modes, are found in both FTIR spectra of UIO-66 and UIO-S_{0.6} [24]. In contrast, the enhanced band at 1245 and 1170 cm⁻¹ are assigned to symmetric SO₂ stretching mode in UIO-S_{0.6} catalyst, confirming the functionalization of the UIO-66 frameworks by sulfonic groups (Table S3) [25].

In order to explore deep insight into Lewis and Brønsted acid sites of UIO-S_{0.6} catalyst, pyridine adsorption FTIR was performed at various temperatures (150, 225, and 275 °C). According to the literature, vibrational bands at 1445 and 1606 cm⁻¹ were assigned to Lewis acid, 1540 cm⁻¹ band was attributed to Brønsted acid, and 1490 cm⁻¹ band was assigned to both Lewis acid and Brønsted acid [26,27]. The Lewis acid originated from metal Zr centers, and the Brønsted acid originated from the -SO₃ functional group and terephthalic acid in the Zr-base metal-organic framework. As shown in Fig. 2(c), the quantitative analysis (in-situ FTIR for pyridine adsorptipn) suggested the amount of Brønsted acid in UIO- $S_{0.6}$ are 9.06 µmol g^{-1} and Lewis acid are 36.16 µmol g^{-1} at 150 °C, which are much higher than UIO-66. When the temperature further increased to 275 °C, a decrease in above bands is attributed to the desorption of pyridine at high temperature. Strong strengthen and high density of acidity in UIO-S_{0.6} were favorable for facilitating the adsorption and activation of the -CHO functional groups in aldehydes and -OH functional group in IPA, enhancing the CTH reaction.

To identify the coordinatively unsaturated Zr sites, *in-situ* CO-FTIR adsorption on UIO-66 and UIO- $S_{0.6}$ were performed. UIO-66 was firstly annealed at 300 °C under vacuum for 2 h to remove adsorbed water then cooled to 30 °C to provide a clean UIO-66 surface. After the introduction of CO to the sample cell at 150 °C, characteristic bands at 2171 and 2120 cm $^{-1}$, attributed to σ -coordinated CO on Zr with different strength of Lewis acidic sites, are observed in the spectrum of UIO-66 (Fig. 2d) [21,28]. When CO adsorbed on UIO- $S_{0.6}$ catalyst under identical conditions, bands at 1857, 1822, 1972, and 2026 cm $^{-1}$, attributed to bridge-bound CO (CO_B), unidentate carboxyl species (COOH_L), linearly bound CO (CO_L), respectively, were observed. The shift of Lewis acid sites band from UIO-66 to the bridge-bound and linearly bound on UIO- $S_{0.6}$ catalysts demonstrated the different acid-base properties between UIO-66 and UIO- $S_{0.6}$.

The CTH of FF in IPA was employed to examine the catalytic performance of various catalysts, and the results were depicted in Fig. 3(a). The blank run showed that the CTH reaction did not proceed without any catalyst at the identical condition (Fig. 3a, Table S5). Then, Lewis acidic Zr-base salts (ZrCl₄, ZrSO₄, and ZrClO₂) and ZrO₂ shows low catalytic performance in the CTH of FF into

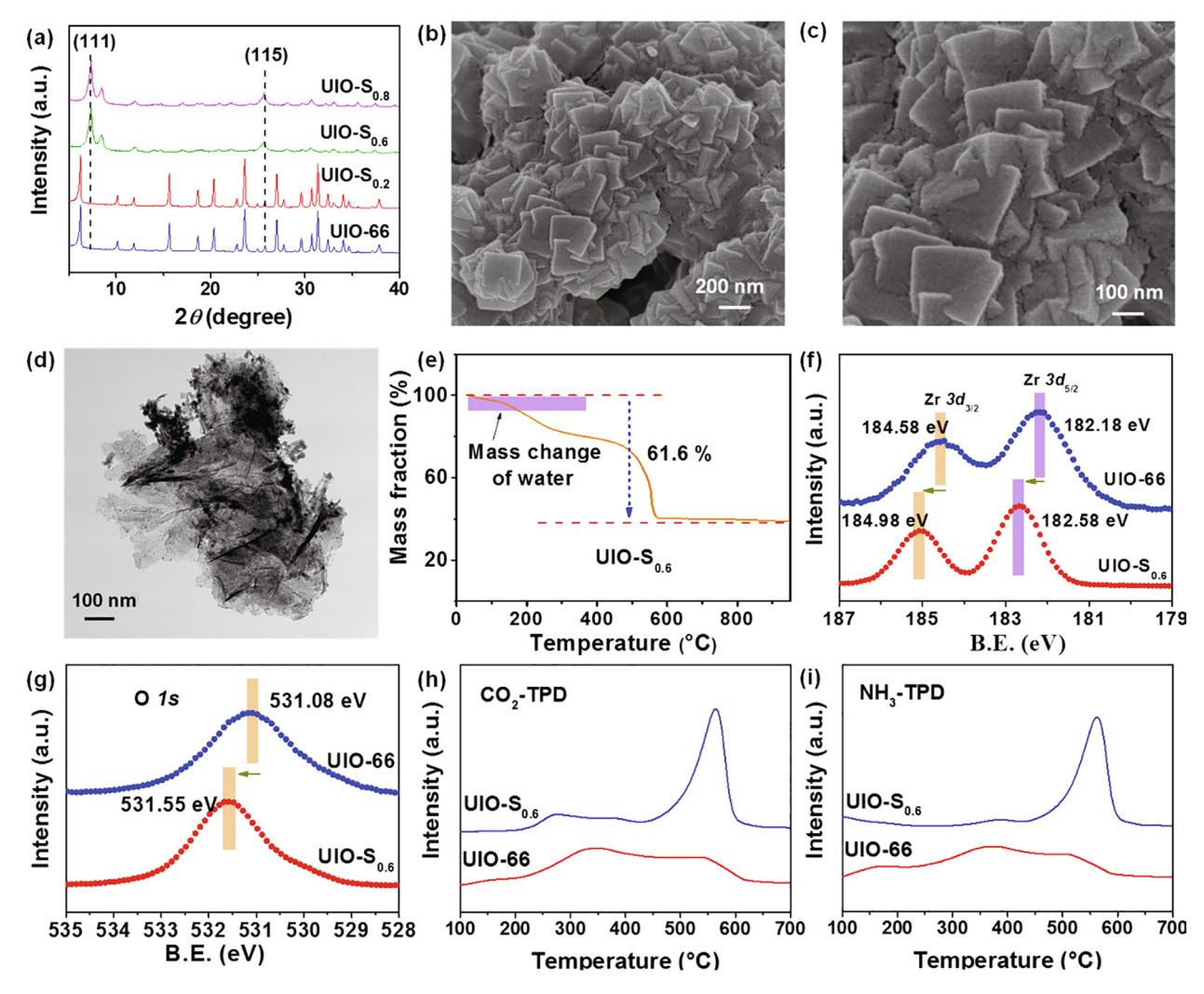


Fig. 1. (a) XRD patterns of UIO-66 and UIO- S_{x_t} (b and c) SEM and (d) TEM image of UIO- $S_{0.6}$, The XPS spectra of (e) Zr 3d and (f) O 1s for UIO-66 and UIO- $S_{0.6}$, (g) TG curve of UIO- $S_{0.6}$, (h) CO₂-TPD, and (i) NH₃-TPD of UIO-66 and UIO- $S_{0.6}$.

FOL, the main by-product is the acetalization of FF with IPA into furfural diisopropyl acetal (FDIA). Besides, the conventional UIO-66 only gave 21.8% FOL yield and 5.2 h⁻¹ turnover number (TOF). The low FOL yield and TOF may be attributed to the weak Lewis acidic sites of UIO-66. After sulfonic groups functionalized UIO-66, the FOL yield increased from 21.8% to 73.2% after the UIO-66 was functionalized by sulfonic groups. Moreover, the transformation of FOL was remarkably from 73.2% to 94.2% as the ratio of -SO₃H to Zr increased from 0.2 to 0.6. However, further elevating -SO₃ loading amounts has only slightly improved the FOL yield. This is attributed to the amount of -Zr-O species in UIO-66 is constant. Besides, other functionalized metal-organic frameworks exhibit a lower FOL yield and TOF than UIO-S_{0.6} catalysts, and the primary side product was the transesterified products between FF and IPA. Combined with the detailed characterizations and the experimental results, it assumed that the acidic and basic sites with appropriate density and strength in the above catalysts are the critical factors for the selective CTH of FF to FOL. As discussed above, the contents of the acidic and basic sites of UIO-S_{0.6} catalyst were stronger than UIO-66 and UIO-S_{0.6} by analyzing the results of NH₃-TPD and CO₂-TPD. Therefore, we assume that the presence of both basic and acidic sites with appropriate content and strength in the prepared catalysts are the key factors for the selective conversion of FF into FOL combining with the catalysts characterizations and the activity tests. In order to elucidate our assumption

and obtain more profound insight into the role of the acid-base properties in the CTH reactions, benzoic acid, pyridine, and 2,6-lutidine were employed as poisoning additives in the reaction. When 50 mg benzoic acid was added to the reaction, a drastic decrease in FF conversion and FOL yield was observed, suggesting the CTH reaction closely depends on the basic sites (Fig. 3b, Table S5). A slight decrease in FF conversion and FOL yield when adding pyridine to the reaction, suggests acid sites are also beneficial for the CTH reactions. To further identify the role of acid sites (Lewis and Brønsted acid) on the FF CTH, 2,6-lutidine was employed as an additive to selective poison Brønsted acid. A slight decrease in FOL selectivity is observed, suggesting Brønsted acid sites can helpful for the CTH of FF. The poisoning experiments demonstrated that both Lewis acidic-basic and Brønsted acidic sites are essential for the selective CTH of FF into FOL.

The solvent is the hydrogen donor for the CTH of FF to FOL. The effect of solvent on the CTH of FF over UIO-S_{0.6} catalyst was conducted, and the results were depicted in Fig. 3(c) and Table S6. Both primary and secondary alcohols have the ability to CTH of FF into FOL. Particularly, secondary alcohols exhibit better catalytic performance than primary alcohols (Fig. 3c, Table S6). The primary side reaction is the acetalization of FF and IPA. Besides, with an increase of the carbon chain of alcohols, a slight decrease in FOL selectivity was observed. It is because the long-chain alcohols have a significant negative steric effect, hindering the diffusion of FF molecules into

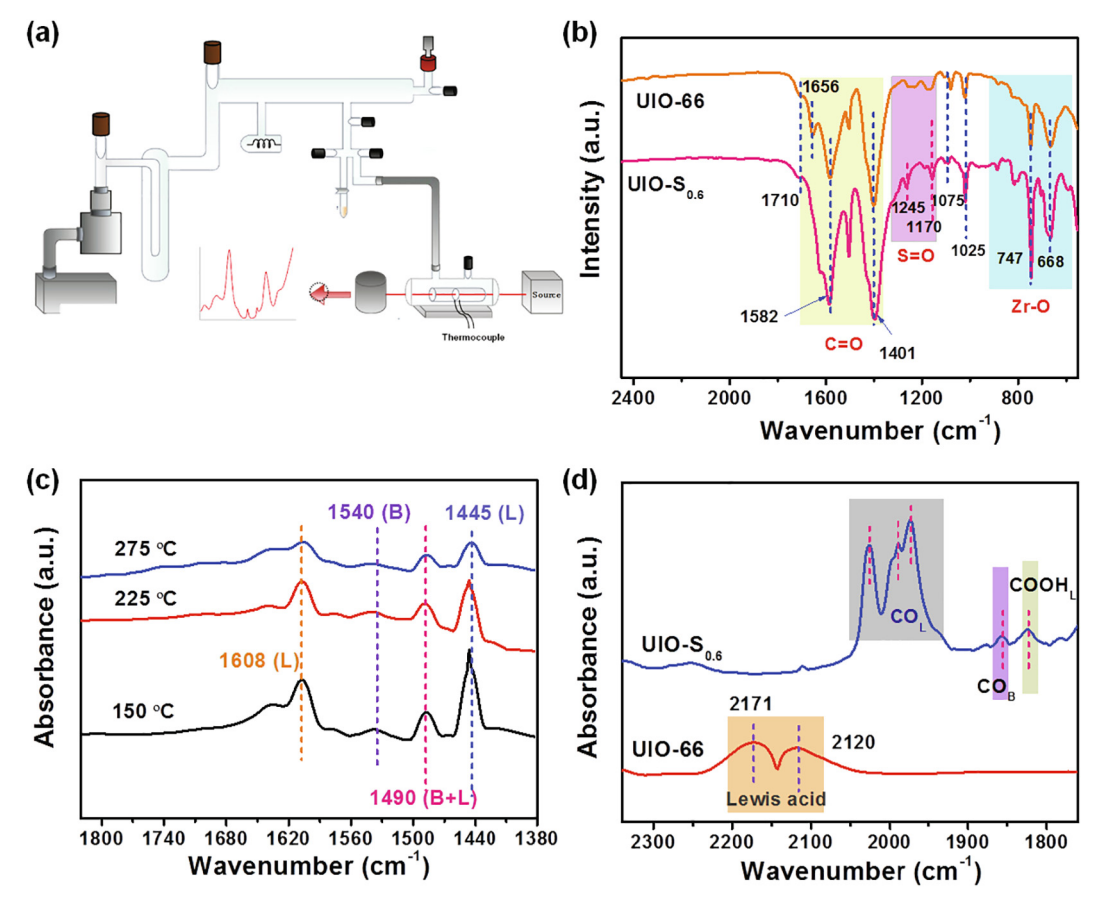


Fig. 2. (a) The schematic diagram for *in-situ* transmission FTIR; (b) transmission FTIR spectra of UIO-66 and UIO-S_{0.6}; (c) transmission FTIR spectra of UIO-S_{0.6} after the adsorption of pyridine at various temperatures; (d) CO-FTIR adsorption on UIO-66 and UIO-S_{0.6}.

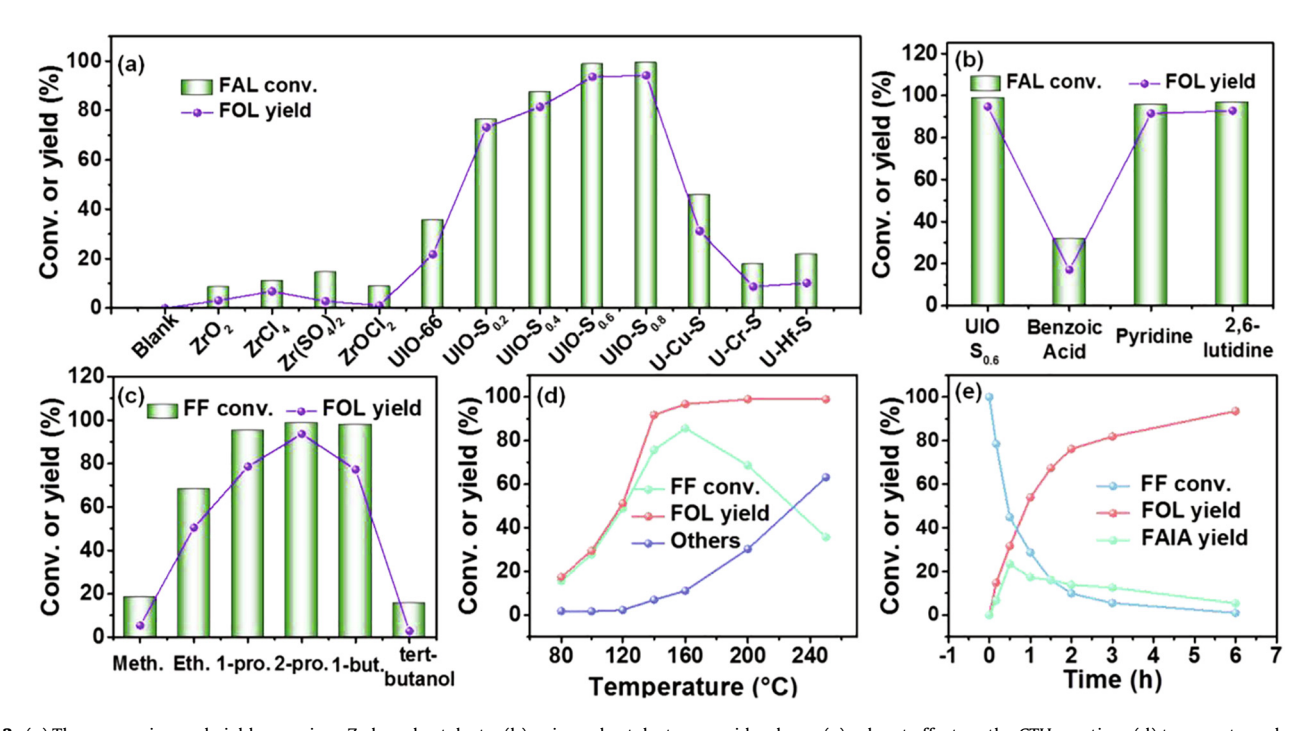


Fig. 3. (a) The conversion and yield on various Zr-based catalysts; (b) poisoned catalyst over acid or base; (c) solvent effect on the CTH reaction; (d) temperature-dependent product distributions; (e) time course and the product distributions in the CTH of FF with IPA. Reaction conditions: 0.5 mmol FF in 5 mL IPA, 50 mL catalyst or 22% mol metal catalyst.

the channels of UIO-S $_{0.6}$. However, when tert-butanol was employed as the solvent and hydrogen donor, a low FF conversion was obtained, suggesting the presence of β -H in alcohols is indispensable for the CTH of FF. Therefore, IPA was the best solvent for the hydrogen donor and was chosen for the CTH reactions.

Furthermore, the influence of temperature on the CTH of FF over $UIO-S_{0.6}$ catalyst was investigated. As depicted in Fig. 3(d), the reaction temperature played a crucial role in the activity and selectivity. When the CTH reaction was conducted at 80 °C, only 15.6% FOL yield was obtained, suggesting higher temperature is indispensable to activate the IPA and FF. When reaction temperature increased to 140 °C, the conversion of FF dramatically increased to 91.8% with a high FOL selectivity since it is prone to promote the hydrogen transfer from IPA to FF at higher temperature. However, when the reaction temperature reaches 250 °C, a significant decrease in FOL selectivity with an increase in FF conversion was observed, suggesting side reactions occurred at high temperatures. The main side reaction was self-condensation, hydrogenolysis, decarbonylation and hydrodeoxygenation of FF, which were confirmed by gas chromatograph-mass spectroscopy (GC-MS) (Fig. S4). Among these side products, 2-methylfuran, furan, 2methyltetrahydrofuran, cyclopentanol are high-quality biofuels

and additives. To obtain the desired products, FOL, $150\,^{\circ}\text{C}$ was chosen as the best temperature for the further CTH reactions.

The time course of CTH of FF over UIO- $S_{0.6}$ catalyst was performed to explore the reaction pathway at 150 °C (Fig. 3e). It can be seen that FF was converted entirely, and 93.6% FOL yield was obtained at 150 °C for 6 h. FDIA was the only side product in the CTH reaction. The side products FDIA increased at the first 0.5 h and then declined with the increase in the FOL yield. It is proposed that there are two pathways for the CTH of FF: (1) FDIA is not stable, and it could be reversibly converted to FF and IPA, finally converted to FOL via CTH pathway; (2) FDIA is an intermediate and can be directly transferred to FOL.

In order to explore the relationship between active sites of the as-prepared UIO-S $_{0.6}$ catalyst and their catalytic performance, kinetic experiments were conducted. The experiments were performed with 20, 35, and 50 mg catalyst at low reaction temperatures (100 °C) to avoid mass transfer limitations. As shown in Fig. S5(a), the mass of catalyst and FOL yield have a linear relationship, implying the FOL formation rate had a first-order dependence on the mass of catalyst. Also, it suggests that the adsorption and activation of FF molecule on UIO-S $_{0.6}$ surface was the rate-determining step.

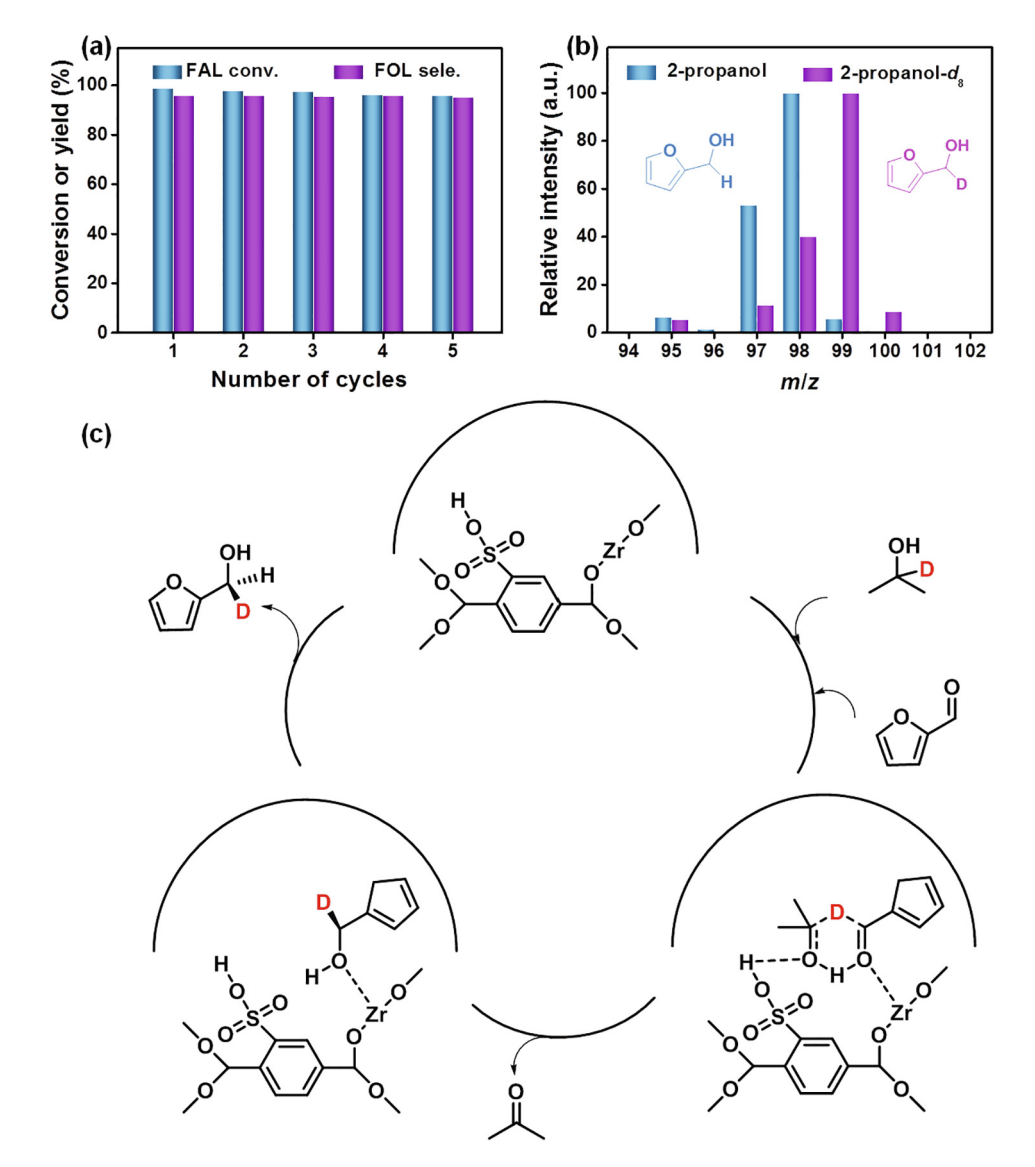


Fig. 4. (a) The stability of the UIO-S_{0.6} catalyst in the CTH of FF. (b) mass spectra of FF obtained after hydrogenation of FF. Reaction condition: 0.5 mmol FF in 5 mL IPA, 50 mg UIO-S_{0.6} catalyst, 3 h. (c) Possible mechanism for the CTH of FF to FOL over UIO-S_{0.6} catalyst.

To further study the apparent activation energy (E_a) of the FF hydrogenation, kinetic experiments were investigated over 373, 393, and 413 K. The rating formula of FF CTH was expressed in Eq. (1), where c_0 is the initial concentration of FF and c_t is the concentration of FF after a reaction time t. Because of the fixed mass of catalyst and the excess of a hydrogen donor, we assumed that the CTH reaction was the first order as a function of the FF concentration (γ = 1). Therefore, Eq. (1) can be expressed to Eq. (2) or Eq. (3). The Arrhenius plots in the CTH of FF over UIO-S_{0.6} catalyst were depicted in Fig. S5(b). The apparent activation energy on UIO-S_{0.6} was as low as 50.8 kJ mol⁻¹. which is lower than the previous work (Table S7).

$$-\frac{\mathrm{d}c(\mathrm{FAL})}{\mathrm{d}t} = kc(\mathrm{FAL})^{\partial} \tag{1}$$

$$\ln \frac{c_t}{c_0} = -kt \tag{2}$$

$$\ln k = \ln A - \frac{E_{\rm a}}{RT} \tag{3}$$

The stability of catalysts is essential for determining the potential value of catalysts in industry application. The recycling experiments of UIO-S_{0.6} for the CTH of FF were performed at 150 °C for 6 h (Fig. 4a). After the first run, the UIO- $S_{0.6}$ catalyst was separated by centrifugation and then was washed with ethanol 3 times and dried at 60 °C overnight. Because of the loss of catalysts, a small scale of FF CTH experiments was performed to stay the same ratio of the substrate, solvent, and catalyst at every cycle. The FF conversion decreased from 98.7% to 95.8% after five cycles, suggesting the excellent reusability of UIO-S_{0.6} catalysts. The catalyst after stability testing was characterized by XRD and ICP. The XRD patterns suggested that the amorphous morphology of the UIO-S_{0.6} catalyst remained as a fresh catalyst (Fig. S6). Furthermore, the IPC results indicated that only a small amount of S and Zr were leaching after five cycles of experiments. The slight decrease in the FF conversion and FOL selectivity may be attributed to the loss of the acidic-basic active site (Zr and S).

There are two mechanisms for the reduction of FF to FOL, and the main difference between those two hydrogenation mechanisms is whether the direct adsorption of H on the catalyst (Fig. S7). The CTH mechanism proceeded by forming a sixmembered ring, and then the β -H of the IPA donor was transferred to the carbonyl carbon of FF. The H did not adsorb on the catalyst surface in the CTH mechanism (Fig. S7a). In contrast, the metalmediated mechanism included two steps (Fig. S7b) [21,29]. First, IPA was dehydrogenated on the metal sites and formed the adsorbed H and acetone, then the transformation of the H atom to the -CHO functional groups. The H atoms were adsorbed onto the metal sites and then transferred to the -CHO functional groups in the metal-mediated mechanism. However, using deuterated 2-IPA- d_8 to replace 2-IPA- d_0 cannot differentiate these two mechanisms because the formed FOL had identical isotopic structure via either mechanism.

Therefore, isotopic labeling experiments in IPA- d_0 and deuterated IPA- d_8 with in excess tert-butanol were performed to study the CTH of the FF reaction mechanism over the UIO- $S_{0.6}$ catalyst. In the study, tert-butanol was employed because for two reasons: (1) the lack of β -H could prevent the CTH mechanism, which is proved in the solvent effects (2) the presence of H in the –OH functional group could exchange with the active H on the surface of the catalyst while leaving the H atom in the C–H bond untouched. In the mixture of IPA- d_8 and tert-butanol, tert-butanol is in great excess with respect to IPA- d_8 , and most of the OD in IPA- d_8 will be exchanged into OH because of the fast OH/OD exchange between alcohols. Thus, IPA- d_7 (CD₃CD(OH)CD₃) is the majority

of the D (or H) donor when the mixture solution (5 wt% IPA-d8 and 95 wt% *tert*-butanol) is used. The GC-MS fragmentation pattern of FOL produced with IPA- d_0 as the hydrogen donor at 150 °C matched well with the NIST database (Fig. S8). The most intense peak was the parent ion of FOL (98 amu) in the blue bar (Fig. 4b), a small signal in 99 amu was observed due to the natural isotope abundance of 13 C. A clear 1 amu mass shift was shown in Fig. 4b (purple bar) when IPA- d_8 with in excess *tert*-butanol was employed as hydrogen donor under the same reaction conditions, suggesting the concerted intermolecular hydride transfer mechanism is the main reaction pathway in the hydrogenation of FF into FOI

Combined with the physicochemical characterization, catalytic performance of catalysts, poisoning experiments, kinetic studies, and isotopic labeling experiments, we proposed the reaction mechanism for the CTH of FF over UIO-S_{0.6} catalyst in Fig. 4(c). Firstly, the dissociative adsorption IPA on the surface of UIO-S_{0.6} catalyst to form the corresponding alkoxide and hydrogen via the Lewis acidic-basic sites (Zr⁴⁺-O²⁻). Meanwhile, the deprotonation of IPA was promoted by the basic site (O²⁻). The –CHO functional group in the FF molecule was activated by the Lewis acidic-basic sites (Zr⁴⁺ or sulfonic functional groups) and Brønsted acidic sites (–SO₃H). Then the transition state (six-membered ring) was formed with –CHO group and IPA, resulting in the direct hydride transfer by β -H elimination and producing the corresponding alcohols.

3. Conclusions

In summary, an efficient UIO-S, catalyst for the CTH of FF to FOL was prepared by modified UIO-66 by sulfonic groups without changing the organic framework. The resulting catalyst UIO-S_{0.6} exhibit excellent catalytic performance of 94.7% FOL yield and 16.9 h⁻¹ TOF under mild conditions. It was found that strong interaction between Zr and terephthalic acid hydroxyl groups led to the formation of strong Lewis acidic and basic sites in the organic frameworks. Mechanism studies demonstrated the cooperative role of strong Lewis acidic and basic sites in the modeified UIO-S_{0.6} catalyst contributed to the excellent catalytic performance in the CTH reaction. Kinetic experiments indicated that the activation energy of the CTH of FF over UIO- $S_{0.6}$ was as low as 50.8 kJ mol⁻¹. Isotopic labeling experiments elaborated that the β -H in IPA was transferred to the α -C of FF by forming six-membered intermediates on the Lewis acidic-basic and Brønsted acidic sites of the UIO-S_{0.6}, and then the β -H was transferred to the α -C of FF, which is the rate-determining step in the formation of FOL. Besides, the recycling experiments suggested that the UIO-S_{0.6} can be reused at least five times without significant change. This work provides a promising strategy to modify the acid-base properties of UIO-66 without affecting its structure. Moreover, the mechanistic insights in identifying the active sites (acid-base properties) on the catalytic performance may guide future catalyst design.

Declaration of competing interest

The authors declare that they have no known competing financial interests or personal relationships that could have appeared to influence the work reported in this paper.

Acknowledgments

This work was supported by the National Key R&D Program of China (2020YFA0710000), the National Natural Science Foundation of China (22122901, 21902047), the Provincial Natural Science Foundation of Hunan (2020][5045, 2021][20024, 2021RC3054),

and the Shenzhen Science and Technology Program (JCYJ20210324140610028). The authors sincerely thank Suzhou Deyou Bot Advance Materials Co., Ltd. and Prof. Wentai Wang for providing support on material characterization.

Appendix A. Supplementary data

Supplementary data to this article can be found online at https://doi.org/10.1016/j.jechem.2022.02.047.

References

- [1] E.L. Kunkes, D.A. Simonetti, R.M. West, J.C. Serrano-Ruiz, C.A. Gärtner, J.A. Dumesic, Science. 322 (2008) 417–421.
- [2] N. Zhang, Y. Zou, L. Tao, W. Chen, L. Zhou, Z. Liu, B. Zhou, G. Huang, H. Lin, S. Wang, Angew. Chem. Int. Ed. 58 (2019) 15895–15903.
- [3] J. Wu, Q. Chen, L. Chem, Q. Liu, C.G. Wang, L.L. Ma, Energ. Fuels. 34 (2020) 2178–2184
- [4] Y. Lu, C. Dong, Y. Huang, Y. Zou, Z. Liu, Y. Liu, Y. Li, N. He, J. Shi, S. Wang, Angew. Chen. Int. Ed. 59 (2020) 19215–19221.
- [5] B. Zhou, C. Dong, Y. Huang, N. Zhang, Y. Wu, Y. Lu, X. Yue, Z. Xiao, Y. Zou, S. Wang, J. Energ. Chem. 61 (2021) 179–185.
- [6] Y. Lu, T. Liu, C. Dong, Y. Huang, Y. Li, J. Chen, Y. Zou, S. Wang, Adv. Mater. 33 (2021) 2007056.
- [7] J. Wu, B. Murphy, N. Gould, C. Wang, L. Ma, B. Xu, ChemCatChem 11 (2019) 3254–3263.
- [8] H. Zhao, J.E. Holladay, H. Brown, Z.C. Zhang, Science 316 (2007) 1597-1600.
- [9] Z. Zhang, Q. Wang, H. Xie, W. Liu, Z. Zhao, ChemSusChem 4 (2011) 131-138.

- [10] J. Wu, C. Liu, Y. Zhu, X. Song, C. Wen, X. Zhang, C. Wang, L. Ma, J. Energ. Chem. 60 (2021) 16–24.
- [11] J.H. Wang, F.H. Richter, F. Wang, H.J. Bongard, B. Spliethoff, C. Weidenthaler, F. Schüth, Nat. Mater. 13 (2014) 293–300.
- [12] Y. Fan, C. Zhuang, S. Li, Y. Wang, X. Zou, X. Liu, W. Huang, G. Zhu, J. Mater. Chem. A 9 (2021) 1110–1118.
- [13] Y. Wang, R. Liang, K.S. Triantafyllidisef, W. Yang, C. Len, Mol. Catal. 499 (2021) 111199.
- [14] N.S. Gould, B. Xu, Chem. Sci. 9 (2018) 281-287.
- [15] J. Zhang, Z. Qi, Y. Liu, J. Wei, X. Tang, L. He, L. Peng, Energ. Fuel. 34(2020) 8432–8439.
- [16] M.L. Koehle, R.F. Lobo, Catal, Sci. Technol. 6 (2016) 3018-3026.
- [17] S.H. Zhou, F.T. Dai, Y.A. Chen, C. Dang, C.Z. Zhang, D.T. Liu, H.S. Qi, Green Chem. 21 (2019) 1421–1431.
- [18] A.H. Valekar, M. Lee, J.W. Yoon, J. Kwak, D.Y. Hong, J. Jung, J.S. Chang, Y.K. Hwang, ACS Catal. 10 (2020) 3720–3732.
- [19] L. Gao, G. Li, Z. Sheng, Y. Tang, Y. Zhang, J. Catal. 389 (2020) 623-630.
- [20] Y.K. Kuwahara, W.Y. Osada, T. Fujitani, H. Yamashita, Catal. Today 281 (2017)
- [21] J.Z. Song, H. Zhou, L. Wu, Q. Meng, Z. Liu, B. Han, Angew. Chem. Int. Ed. 54 (2015) 9399–9403.
- [22] B.X. Matthew, J. Gilkey, ACS Catal. 6 (2016) 1420-1436.
- [23] J.Y.F. Lee, O.K.J. Roberts, K.A. Scheidt, S.T. Nguyen, J.T. Hupp, Chem. Soc. Rev. 38 (2009) 1450–1459.
- [24] S.S. Ling, B. Slater, Chem. Sci. 7 (2016) 4706-4712.
- [25] H. Zhang, W. Yang, I.I. Roslan, S. Jaenicke, G.K. Chuah, J. Catal. 375 (2019) 56-67.
- [26] M.L.H. Foo, T. Fukushima, Y. Hijikata, Y. Kubota, M. Takata, S. Kitagawa, Dalton Trans. 41 (2012) 13791–13794.
- [27] L. Valenzano, B. Civalleri, S. Chavan, S. Bordiga, M.H. Nilsen, S. Jakobsen, K.P. Lillerud, C. Lamberti, Chem. Mater. 23 (2011) 1700–1718.
- [28] B.M. Murphy, M.P. Letterio, B. Xu, ACS Catal. 6 (2016) 5117-5131.
- [29] M.J. Gilkey, A.V. Mironenko, G.R. Jenness, D.G. Vlachos, B. Xu, ACS Catal. 5 (2015) 3988–3994.